Measuring and Simulating the Antenna Patterns of ISU's Ground Station

Author: Tingwei Guo

Advisor: Joachim Köppen

Aliakbar Ebrahimi

International Space University

Master in Space Science 2013

Abstract

This report summarizes the work of my individual project which I have done in 2013. The ground station of the International Space University has two stacked Yagi-Uda antennas, their operating frequencies are 144MHz and 432MHz. The subject of my individual project is to simulate and measure the antenna pattern of the two antennas. This report gives the results of measured geometry of the antennas, the manner of antenna modelling, the models of antennas, the simulated antenna patterns, and the measured antenna patterns, etc. The measured and simulated patterns have been compared, and their consistence of measured and simulated antenna patterns have been analysed and explained.

The main conclusions of the report are:

1. The primary lobes in measured antenna patterns are very similar to the simulated ones, which indicates that environmental factors have only a small effect on the primary lobe of a measured antenna pattern.

2. The side lobe shape and level of the measured patterns are different from the simulated ones, which is caused by reflecting objects. The main reflective objects are the lightning rod and metal railings.

3. If an antenna has many elements, definition of the model of the antenna through direct edition in the *.MAA file is an efficient way.

Keywords: Yagi-Uda antenna, Simulation, Antenna pattern, Antenna measurement

摘 要

本报告总结了我于2013年在国际空间大学所完成的个人项目的相关工作。国际空间大学的地面站含有两个八木天线阵列，它们工作频率分别是144MHz和432MHz，我的个人项目的内容就是仿真并测量这两个天线的方向图。报告中给出了天线辐射单元参数测量结果，天线建模方法，天线仿真模型，天线方向图仿真结果和天线方向图测量结果，对天线仿真方向图及测量方向图进行了解释说明，并对天线仿真方向图与实际测量方向图进行了对比分析，对其中的异常点进行了分析解释。

本报告主要结论包括：

1. 从仿真结果与实际测量结果对比发现，天线方向图主瓣极为相似，表明环境因素对天线方向图主瓣测量影响很小。

2. 实测天线方向图副瓣形状及副瓣电平与仿真结果差异较大，这是受天线周围反射体影响的结果，主要反射体为避雷针及天线周围的金属栏杆。

3. 当天线辐射单元很多时，通过直接编译仿真软件MMANA-GAL生成的*.MAA文件建模是一个更高效的方法。

关键词： 八木天线，仿真，天线方向图，天线测试

Acknowledgments

Contents

List of Tables

List of Figures

List of abbreviations

HPBW   Half-power beam width

FBR   Front-to-back ratio

H-plane   Horizontal plane

V-plane   Vertical plane

H-polarized   Horizontally polarized

V-polarized   Vertically polarized

AGC   Automatic gain control

ISU   International Space University

UTC   Coordinated Universal Time

dBm   Decibel milliwatt

1. Introduction

1.1. Ground station

The ISU-Ground Station works on the frequencies of 144, 432, and 2400 MHz. Seen in the figure below, the antenna on the left has a working frequency of 144MHz, and the antenna on the right has a working frequency of 432MHz, both of the two are Yagi-Uda antennas, and are the object of simulation and measurement in this project.

Figure 1-1 The ISU Ground Station antenna

The antennas are mounted on an H-frame, which can be rotated 360° in azimuth and 85° in elevation. The servo system is controlled from the interior station, shown in the following figure. On the left there are two very similar instruments, both are used to control the attitude of antenna, the top one for control of the elevation and the bottom one is used to control the azimuth, with their values displayed numerically.

Figure 1-2 The ISU Ground Station's control equipment

On the right of figure 1-2, there is the transceiver which receives the signal from pre-amplifier and outputs the signal strength information to a computer, with software running on the computer to record the information automatically.

1.2. Yagi-Uda antennas

The Yagi-Uda antenna was invented by Dr. Shintaro Uda and Dr. Hidetsugu Yagi in the 1920s. These antennas are widely used in wireless radio communication, television signal receiving, etc.

As the following figure illustrates, the second element in a Yagi-Uda antenna is the only active element, all the other elements interact by receiving and reradiating the electromagnetic energy, acting as parasitic elements by induced currents. The important discovery consisted in realizing that the gain is increased by narrowing the beam width of the dipole alone in a very cheap manner, by the means of simple metallic rod or tube conductors as parasitic elements, which focus the electromagnetic energy into the desired direction.
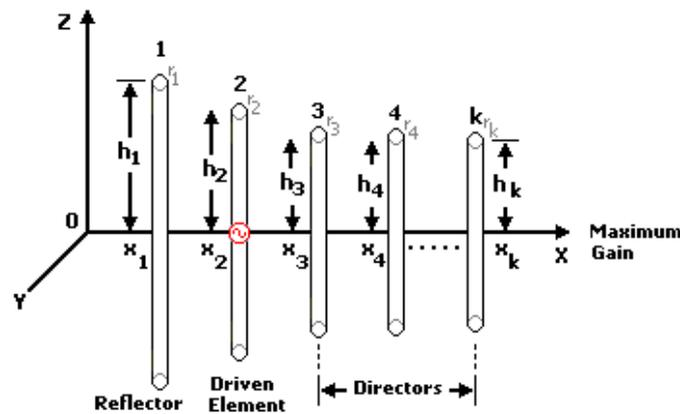
Figure 1-3 Geometry of a Yagi-Uda antenna [online: http://yagi-uda.com/]

1.3. Stacking of antennas

Usually the more elements a Yagi-Uda antenna has the higher is the gain of the antenna, but the more elements it has, the lower is the additional gain that can be obtained from adding another element. Also the more elements the antenna has, the more difficult is its design and mechanical construction. So the number of elements in a Yagi-Uda antenna is limited, seldom more than twenty.

When we need more antenna gain, the available approach is stacking of several antennas into an array, the following figure is a photo of the stacked antenna of the P-18M radar, a 2×8 (2 rows and 8 columns) array.

Figure 1-4   The stacked antenna of P-18M radar   [reference 6]

The following figure shows the change of the antenna pattern, when different stacking arrangements are taken. The red curve is the pattern of a 2×2 stacked antenna, the blue curve is the pattern of a 2×1 stack, compared to the green curve which is the pattern of a single Yagi-Uda antenna. On the left of the figure is the horizontal plane pattern, and on the right of the figure is vertical plane pattern.

We can find that the more Yagi-Uda antennas are in the array, the higher is its gain and the narrower its primary lobe. Because in the 2×1 stacked antenna one Yagi-Uda antenna is above the other, the horizontal pattern remains equal to that of single antenna, but the vertical pattern is narrower. The primary lobe of a 2×2 stacked antenna is narrower in both vertical and horizontal plane.
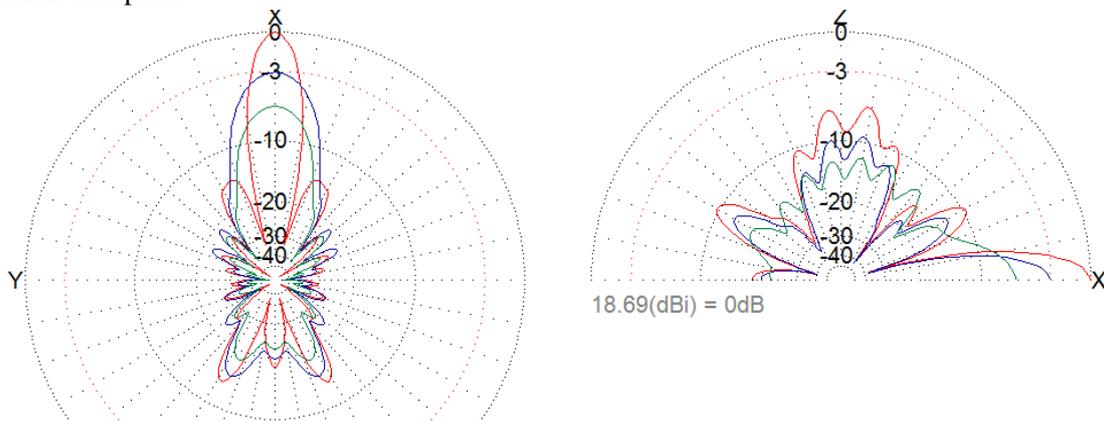
Figure 1-5   The pattern of different stacked antenna

1.4. Environment

Because the antenna of ISU Ground Station is fixed on the roof of ISU building, the actual measurement must be done under this environment. The roof is not an ideal environment for antenna measurement, firstly the position to set up a signal generator is very limited, and any available roof position is lower than the antenna; secondly there are many metal objects in the vicinity such as lightning rod, guardrail, pipes, etc. All these appendages and the platform of

the antenna can reflect electromagnetic waves, and this would affect the results of the measurements. Excepting the actual measurement activity, a great deal of time has been devoted in this project to analyze the influence of these influences.

1.5. Simulation tool: MMANA-GAL

MMANA-GAL is a powerful antenna analysis tool, which based on the moment method (The information about moment method can be found in reference 1, Section 14-11). MMANA-GAL basic is freeware and co-written by Alexandr Schewelev DL1PBD, Igor Gontcharenko DL2KQ and Makoto Mori JE3HHT who also owns the copyright. In this project the software version 'MMANA-GAL basic V.3.0.0.31' is used.

This program has the following functions:
- Table-based editor for antenna design and definition
- Graphical antenna viewer
- Viewer for horizontal and vertical beam radiation patterns
- 3D radiation pattern
- Comparator for two or more "calculation" results
- Antenna element editor
- Antenna wire editor
- Frequency characteristics chart maker
- Data file generator

MMANA-GAL gives us the opportunity to directly observe the model and simulation result of an antenna as shown in figure 3-1.

When we build a model, we can directly input the geometrical descriptions to the table shown as following figure, where X, Y, Z mean the coordinates of the end-points of each element (or 'wire'). If an antenna has a large number of wires, the input all parameters of wires to the table can be laborious. Because the model is described by a normal text file, another efficient manner is edit this '----.maa ' file; it very useful when some wire parameters are the same or similar. The content of the document is shown in chapter 9.

Figure 1-6 Antenna geometry input table

2. Review of related work

2.1. Antenna measurement

Based on different environments antenna measurement can be divided into an anechoic chamber measurement and actual environment measurement.

The following figure is a photo of an anechoic chamber: its walls, ceiling, and floor are covered completely with absorbing material. Thus, the environment in an anechoic chamber is very good approach to a reflection-less free space environment. As the chamber is isolated from interfering signals, it is an ideal environment of antenna measurement.
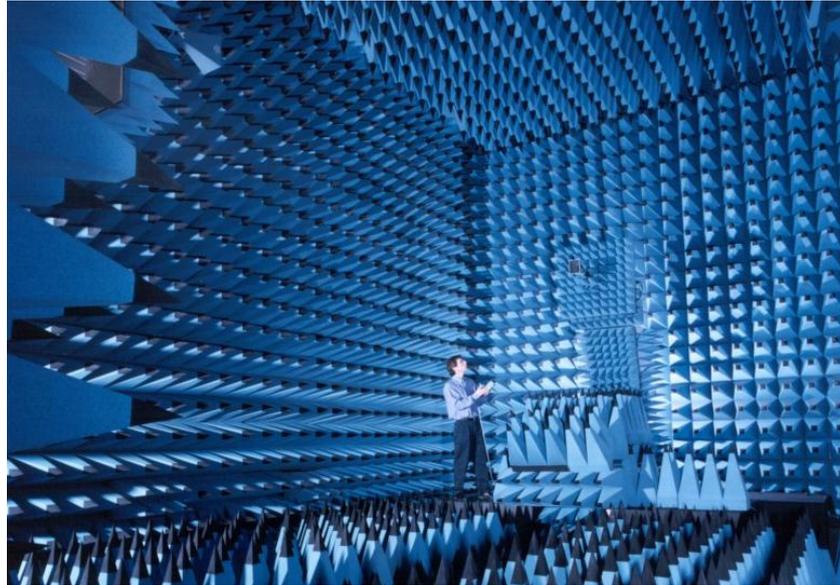
Figure 2-1 Anechoic chamber   [reference 7]

For very large or fixed antennas, the measurement must be done in the actual environment. Usually the antenna of the signal generator is placed on a test tower to reduce the influence from ground reflection.

In anechoic chambers only small high-frequency antennas can be measured at far-field range, but large low-frequency antennas usually can only be measured at near-field range. In actual environments the antenna can usually be measured at far-field range. Far and near fields of an antenna are illustrated in the figure 2-3, where D is the diameter of the smallest stationary sphere enclosing the radiation portions of the antenna as it is rotated for measurement and λ is the wavelength (reference 2 p.95).

The wavelength of ISU Ground Station's 432MHz and 144MHz antennas are 0.7m and 2m, and the D is 3.13m and 3.58m, the corresponding minimum far-field distance are 28.5m and 12.8m. From the scene of measurement as shown in figure 2-2, the distance from ISU Ground Station antenna to signal generator antenna is about 30m (measured with Google Earth), so in this project the antenna measurements are far-field measurements.
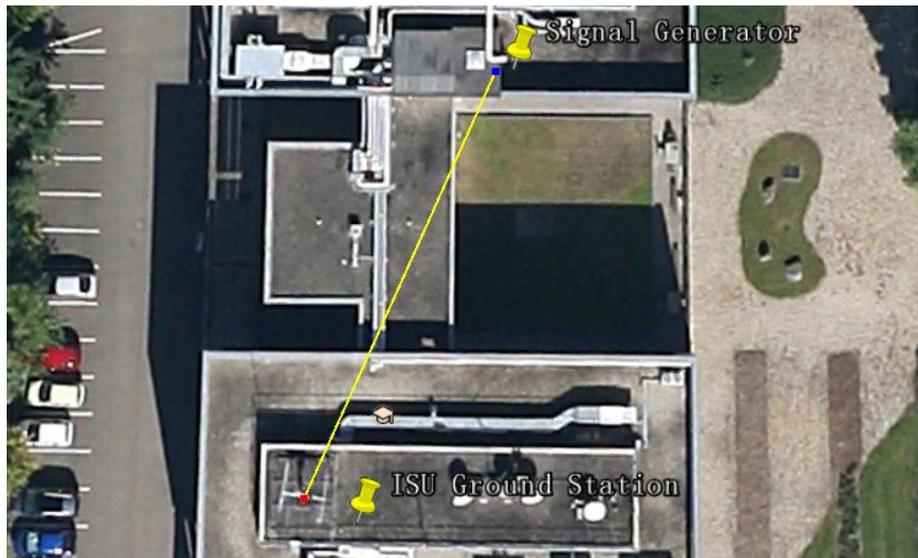
Figure 2-2 The bird's-eye view of ISU building   [Google Earth   update:17/August /2012 access:20/April /2013]
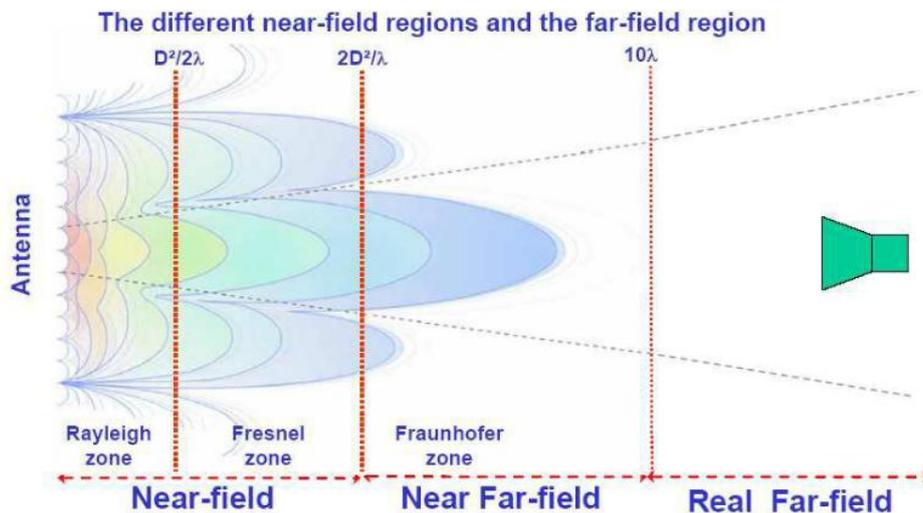
Figure 2-3 The different near-field regions and the far-field region   [reference 8]

2.2. Related work about ISU Ground Station

In 2009, Kaupo Voormansik as one of the first serious user of the ISU Ground Station operated the station to explore its capabilities and measured signal strengths of cubesats. To do so, the whole receive chain of ISU Ground Station was accurately measured and calibrated. For his work some satellites with known emitting power were selected, and through comparison of predicted and actually received signal strengths the performance of the ISU ground station was verified.

In 2011, Fenglei Wu has operated the ISU Ground Station to observe satellites, and measured accurately the overall gain of the station.

3. Methodology

3.1. Method of antenna pattern measurement

The following figure shows a 3-D antenna pattern, which comes from simulation. If we wanted to acquire such a complete pattern through actual measurement, the workload would be very heavy, because if we select angular steps of 5°, we would need to rotate the antenna 1650 times; supposing that one measurement takes one minute, the total time would be 27.5 hours; If we selected the step as 1°, the total time is 688 hours.

Hence most antenna manufacturers or constructors measure the antenna pattern only in the two primary planes, which means the antenna is only rotated in one dimension, while the other dimension (azimuth or elevation) is zero. As this is more efficient and easier to display, but no crucial detail is lost, we selected this method to measure ISU Ground Station antennas.
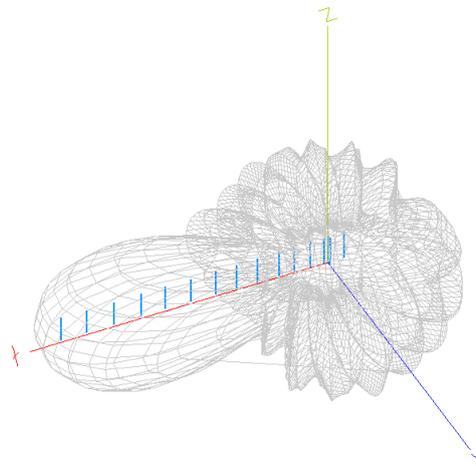
Figure 3-1 Three dimensional antenna pattern

3.2. Processing of measurement data

For antenna pattern measurement we need to record the signal power and the corresponding position angle. As the computer program IC910Tester can only record the signal power as a function of time, I record the azimuth or elevation and time by hand, and then add the azimuth or elevation information to the data document.

To ensure the recorded data is available, the receiver need switched to single-sideband mode (SSB), and the AGC must be set to the fast mode. Because the bandwidth of the receiver is narrow, before recording any data we must carefully adjust the frequency of the receiver system until we hear the signal as a tone of about 1kHz, which means the received signal is in the middle of the receiver's pass band, and during the measurement the tone must be monitored, as if the tone is changed or disappears there must have something wrong, we need to stop and check.

Because the rotators can produce interference noise, especially at the times the start and stop of the rotation, so data processing needs to remove the data recorded during these times. Then the average of those data with same azimuth or elevation can be calculated.

During measurement antenna stayed about 30 seconds on every measuring direction. The raw data looks as follows:

#S-meter readings
#Start at: UT 24.01.2013 08:18:06
#time[UT]   s-value   dBm
08:18:06.411 3 -120.0
08:18:07.646 3 -120.0
08:18:08.880 3 -120.0
08:18:10.114 3 -120.0
        ....
08:25:46.833 146 -89.55
08:25:48.067 146 -89.55
08:25:49.302 146 -89.55
08:25:50.536 146 -89.55
08:25:51.771 146 -89.55
08:25:53.005 39 -116.91
08:25:54.239 3 -120.0
08:25:55.474 3 -120.0
08:25:56.708 3 -120.0
08:25:57.942 3 -120.0
08:25:59.177 168 -79.17
08:26:00.411 168 -79.17
08:26:01.646 168 -79.17
08:26:02.880 168 -79.17
08:26:04.114 168 -79.17

The following figure shows the raw data and processed data . The red curve shows raw data, the green curve shows available valid data, and the blue dot shows the average value of the data with same azimuth and elevation.
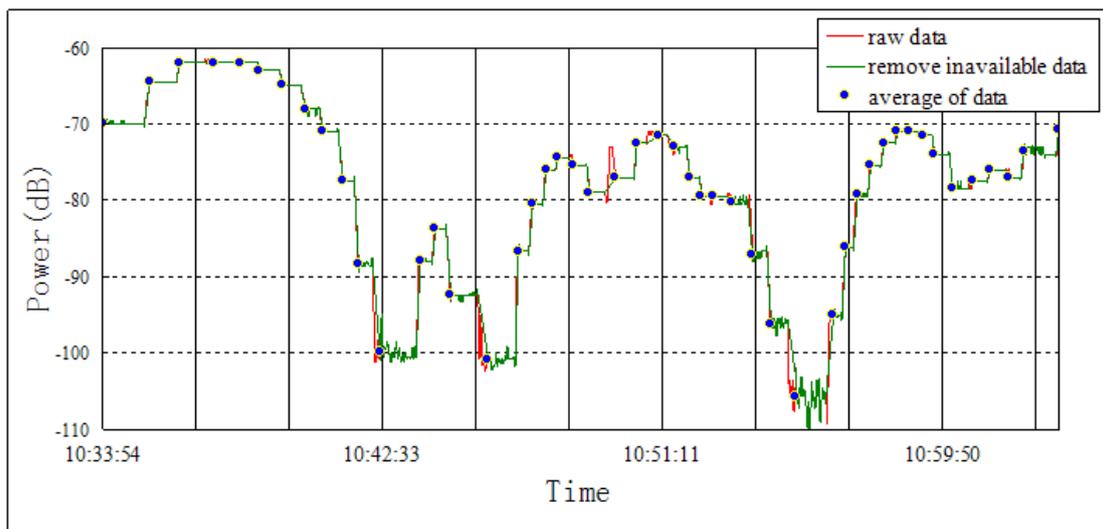
Figure 3-2 Raw and processed data

3.3. Method of multipath simulation

The simulation software MMANA-GAL has functions to automatically form a stacked antenna, and it can rotate antenna to any direction, but as shown in the following figure, when we rotate the automatically formed stack, each Yagi-Uda antenna rotates separately, which is different from the actual rotation of the entire stacked array. In order to form a correct model, we constructed a complete model which includes all wires of a stacked antenna. We find that directly editing the *.maa file is more efficient, the whole model shows in figure 3-4.
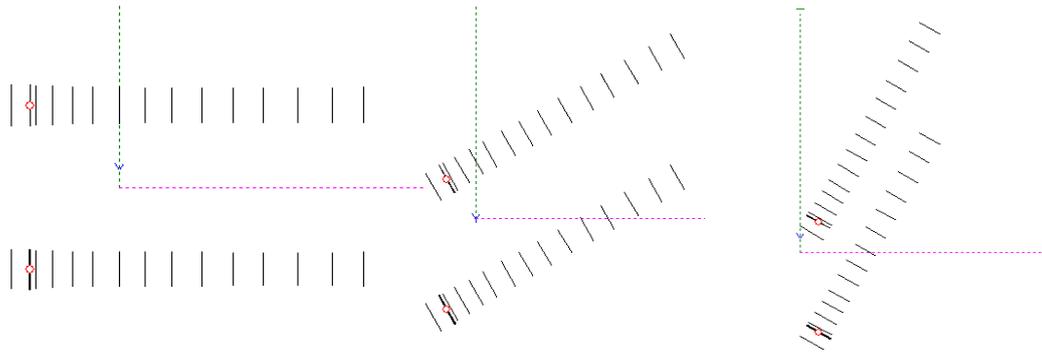
Figure 3-3 The trouble of rotated antennas created by the MMANA-GAL stack option

During the antenna measurement, the antenna is rotated to different directions as shown in figure 3-4. We find that in scenario A, B, and C the relative position of wires and platform are different.

MMANA-GAL calculates the simulated pattern, for which one puts the signal generator at different directions and measures the received signals, so during one simulation the relative position of wires and platform are always the same, which is not consistent to the actual measurements. In order to correctly simulate the antenna, we do many simulations, in every one with the model of antenna is rotated to different directions like in the real measurement. We also need to take into account that the signal generator is slightly below the Ground Station antenna, at an elevation of about -5°. Because MMANA-GAL cannot output correct values for negative elevations, when the platform is included, so in this project the simulated values were collected from the elevation of +3°.

Platform	Platform	Platform
A	B	C
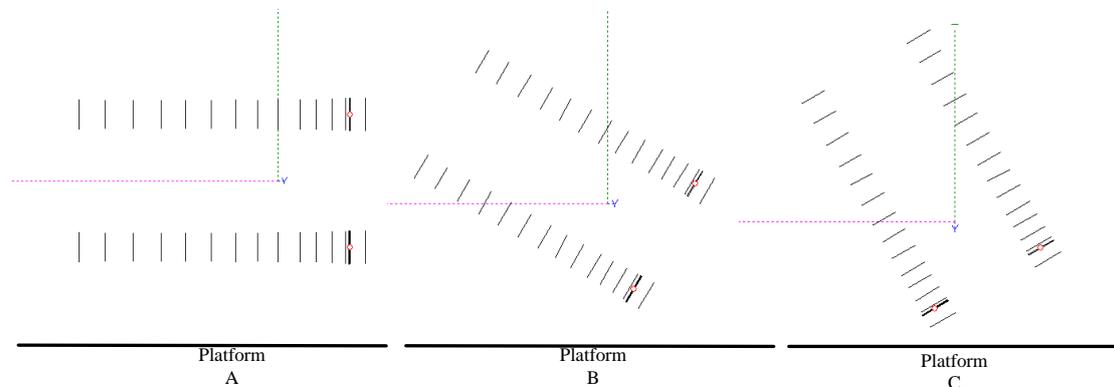
Figure 3-4 The relative position of wires and platform

3.4. Calibration of the measuring software

The receiver of ISU Ground Station can output S-meter codes which give an indication of the strength of the received signal. However the codes must be converted to power values. The converting job is done by the Java software IC910Tester (written by J.K., see Voormansik (2009)), which converts the code into power value and records both values in a file with an accurate time stamp. IC910Tester's working is based on a calibration table, which contains the correspondence between code and power values.

The purpose of calibration is to obtain this calibration table. The manner of calibration is to use a signal generator to input a reference signal to the receiver, and record the power value of the generator and the output S-meter codes of receiver. The procedure of calibration is to gradually increase the signal generator output power, from -120dBm to -50dBm, by steps of 5dB or 10dB.

These calibration data are put in the text file which the Java software IC910Tester reads when it is started. During measurement operations the software reads the S-meter codes from the receiver, and uses the calibration table to convert the codes into proper power values, in dBm.

4. Results and analysis

4.1. Antenna parameter measurement

Before constructing the model for the ISU Ground Station antenna, the dimensions of all the elements must be measured. So in this project my first important job is measure the antenna hardware.

Both of the two stacked antenna have two Yagi-Uda antennas, each of which has several elements, so there are many details that need to be accurately measured and recorded. In order to do this more easily I have drawn detailed diagrams and tables before the actual measurement. The following diagram shows the detailed information for one antenna, whose parameters need to be measured include: the length and diameter of every wire, the relative position of each wire, and the relative position of the two Yagi-Uda antennas.
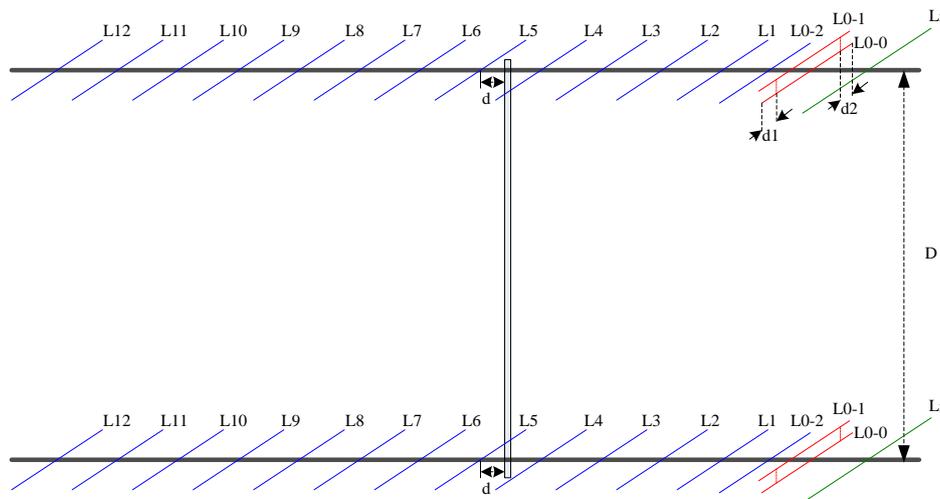
Figure 4-1 The geometry of the 432MHz H-polarized antenna

| Wire | Length(cm) | Diameter(cm) | Distance to L0-0(cm) | | |
			axial direction	Vertical	
L0-0	34.4	0.5	0	0	active
L0-1	31.5	0.3	1	2.7	active
L0-2	31.2	0.5	3.6	0	
Lr	32.6	0.5	15.8	0	
L1	30.5	0.5	17.7	0	
	Length(cm)	Diameter(cm)	Distance to Ln-1(cm)		
L2	29	0.5	14.3	0	
L3	29.4	0.5	15.3	0	
L4	29	0.5	20.9	0	
L5	28	0.5	19.9	0	
L6	28.2	0.5	20.9	0	
L7	28	0.5	24	0	
L8	27.5	0.5	24.4	0	
L9	27.2	0.5	23.7	0	
L10	27.5	0.5	26.5	0	
L11	27.5	0.5	27.1	0	
L12	28.9	0.5	25.2	0	
D	129cm		d1	2.2cm	
D	12.2cm		d2	2.4cm	

Table 4-1 The table to record the geometry measurements

The main tool be used is a ruler and a band tape, the precision of the ruler and band tape is 1mm. Using a ruler to directly measure the diameter of a wire is difficult, so to ensure an accurate result I do it as shown in the following figure, using some elements from the Lego Robot.

The measurement accuracy of relative positions and lengths of wires is lower than the accuracy of the diameter, but all data have an accuracy of magnitude of mm. The wavelength of 432MHz antenna is 0.7m, an error of 1mm is only about 1/700th of the wavelength, which is more than acceptable. The detailed results can be found in chapter 9.
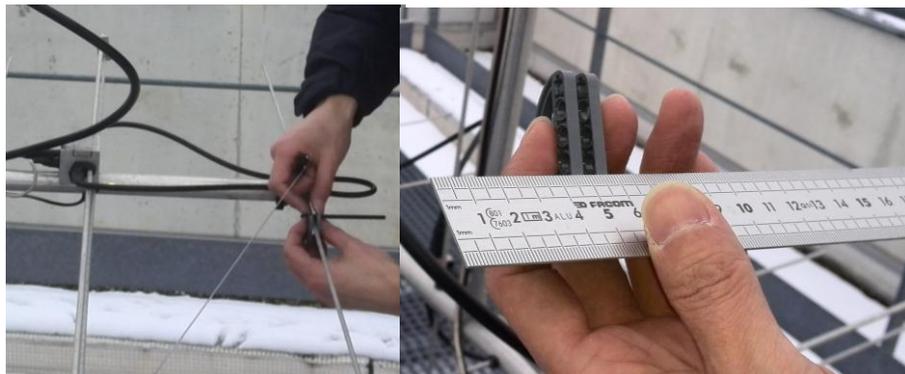
Figure 4-2 Measuring the diameter of a wire

4.2. Antenna pattern simulation

In this section all antenna patterns are simulated under the condition of free space. Models of antennas are constructed based on the results of antenna geometry measurements.

Figures 4-4 to 4-7 are the simulated patterns, on the left of each figure is the H-plane pattern, and on the right is the V-plane pattern.

Figure 4-4 is the simulated pattern of the V-polarized 144MHz antenna. From this we find that the HPBW in the H-plane is about 56°, and about 22° in the V-plane. The HPBW in the V-plane is obviously narrower than in the H-plane, because in vertical dimension there are two stacked Yagi-Uda antennas. The equivalent aperture in vertical dimension is greater than horizontal dimension, and the larger aperture leads to the narrower primary lobe, the similar phenomena can be found in other figures.

Figure 4-5 is the simulated pattern of the H-polarized 144MHz antenna. From this the HPBW in the H-plane is about 46°, and about 22° in the V-plane, and the FBR is 21dB. Compared to Figure 4-3 we find that the HPBW in the H-plane is a bit narrower but in the V-plane it is same. The shape of side lobe is different: the H-polarized antenna has lower side lobes in the H-plane, and the V-polarized antenna has lower side lobes in the V-plane. Similar phenomena can be found in Figures 4-6 and 4-7.

The reason that the H-polarized antenna has a narrower primary lobe than the V-polarized antenna in the H-plane, is the orientation of the elements. The following figure shows that a V-polarized single dipole has an isotropic pattern in the H-plane, but in the V-plane it is non-isotropic and narrower. Because a V-polarized antenna consists of vertical dipoles, it has a relative wider primary lobe and higher side lobe in H-plane than that in V-plane.
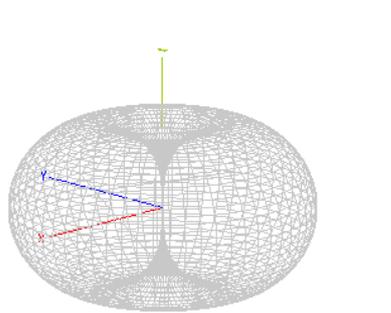
Figure 4-3 The pattern of a V-polarized dipole antenna

Ga : 14.82 dBi = 0 dB (Vertical polarization)
Gh : 12.67 dBd
F/B: 17.51 dB; Rear: Azim. 120 deg, Elev. 60 deg
Freq: 144.000 MHz
Z: 129.618 + j79.497 Ohm
SWR: 3.7 (50.0 Ohm),
Elev: 0.0 deg (Free space)
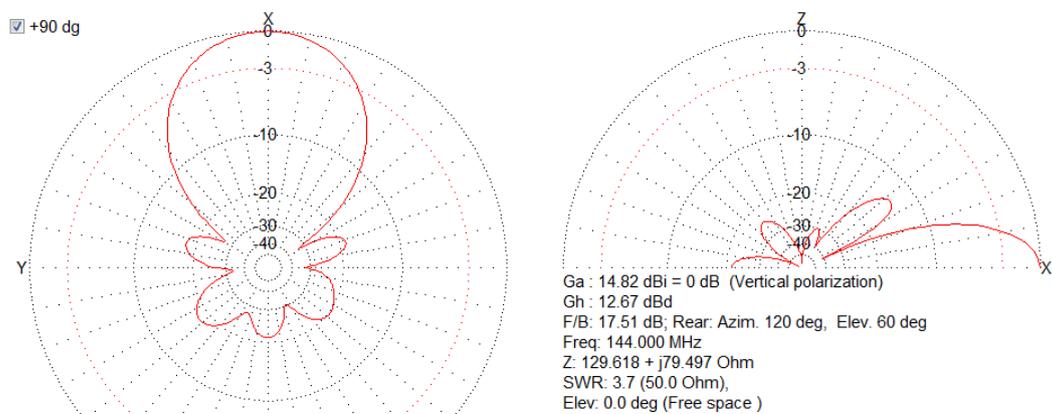
Figure 4-4 The simulated pattern of the V-polarized 144MHz antenna

Ga : 14.47 dBi = 0 dB (Horizontal polarization)
Gh : 12.32 dBd
F/B: 19.75 dB; Rear: Azim. 120 deg, Elev. 60 deg
Freq: 144.000 MHz
Z: 5.437 + j23.284 Ohm
SWR: 11.2 (50.0 Ohm),
Elev: 0.0 deg (Free space)
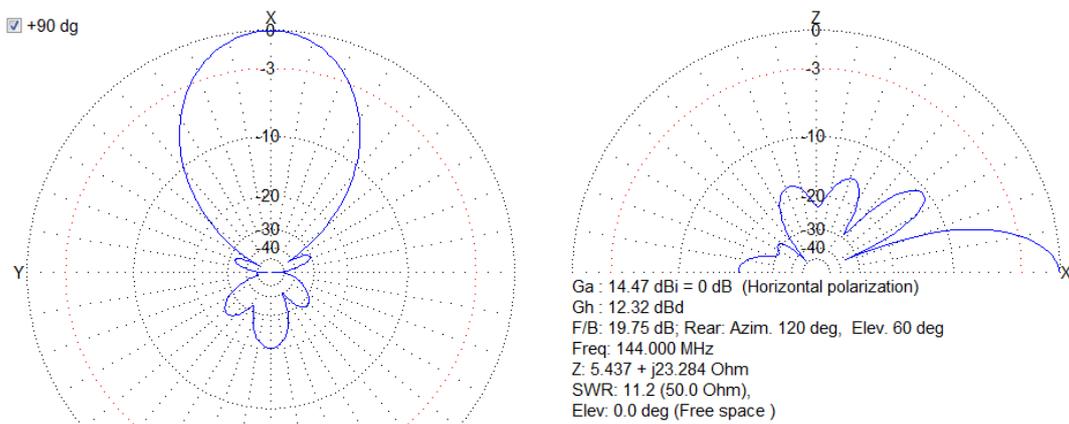
Figure 4-5 The simulated pattern of the H-polarized 144MHz antenna

Figure 4-6 is the simulated pattern of the V-polarized 432MHz antenna. The HPBW in H-plane is about 28°, and about 14° in the V-plane. The FBR is 15dB.

Figure 4-7 is the simulated pattern of the H-polarized 432MHz antenna, with a HPBW in H-plane of about 26°, and about 14° in the V-plane. The FBR is 17dB.

Compared to Figures 4-3 and 4-4, we find that 432MHz antenna has a narrower primary lobe than the 144MHz antenna. This is because the 432 MHz antennas have more wires than 144MHz antennas.

Ga : 16.67 dBi = 0 dB (Vertical polarization)
Gh : 14.52 dBd
F/B: 11.59 dB; Rear: Azim. 120 deg, Elev. 60 deg
Freq: 432.000 MHz
Z: 4.986 + j11.661 Ohm
SWR: 10.6 (50.0 Ohm),
Elev: 0.0 deg (Free space)
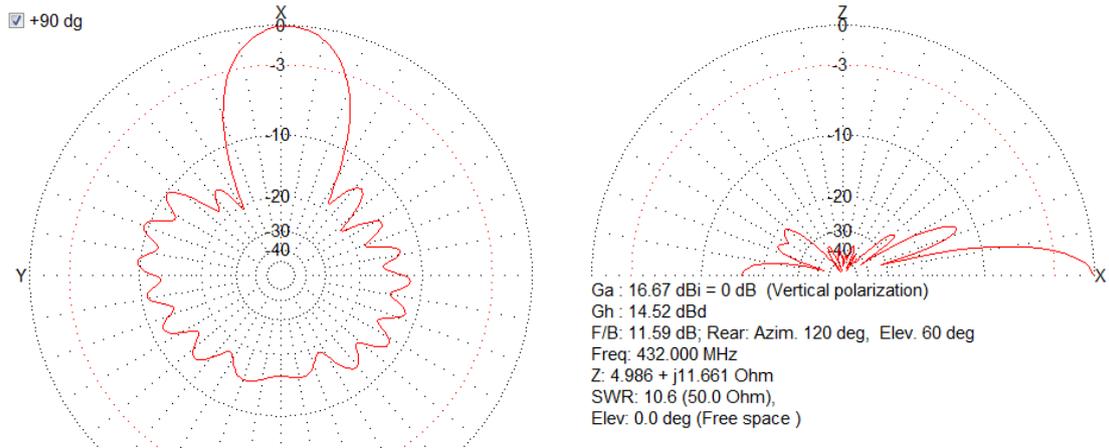
Figure 4-6 The simulated pattern of the V-polarized 432MHz antenna

Ga : 15.65 dBi = 0 dB (Horizontal polarization)
Gh : 13.5 dBd
F/B: 9.20 dB; Rear: Azim. 120 deg, Elev. 60 deg
Freq: 432.000 MHz
Z: 5.170 + j18.640 Ohm
SWR: 11.0 (50.0 Ohm),
Elev: 0.1 deg (Free space)
(For elev. angle 0.0 dg Peak:15.7 dBi)
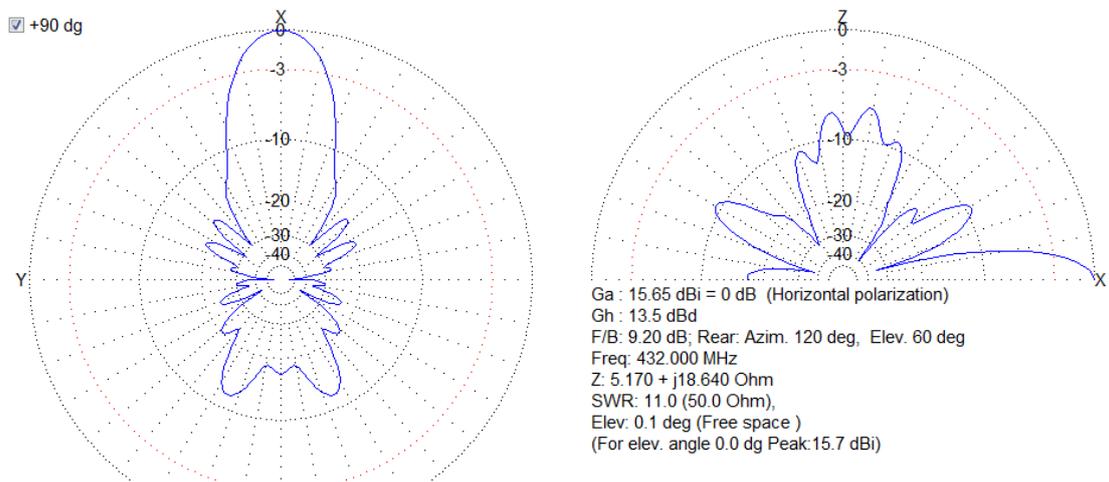
Figure 4-7 The simulated pattern of the H-polarized 432MHz antenna

4.3. Measured antenna pattern in H-plane and comparison

Because the antenna of signal generator is a vertical wire as shown in following figure, the simulation data used for comparison with measured data comes from the V-polarized antenna model.

Figure 4-8 Signal generator and its antenna

Figures 4-9 and 4-10 are comparisons of measured and simulated pattern in the H-plane. Simulated patterns were computed under the condition of 'free space', which means no reflection.
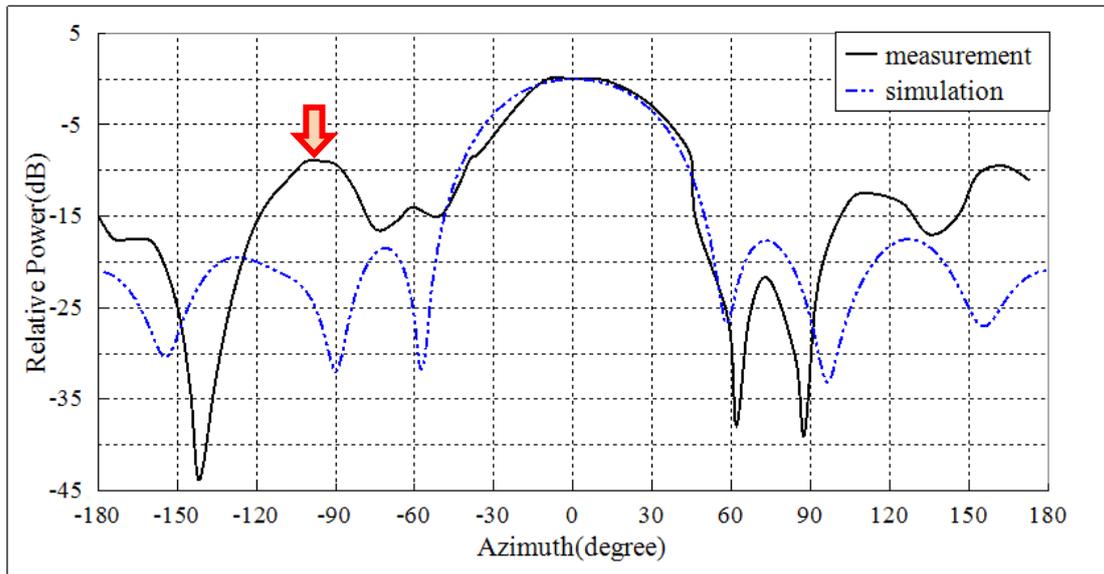
Figure 4-9 H-plane pattern comparison of the V-polarized 144MHz antenna
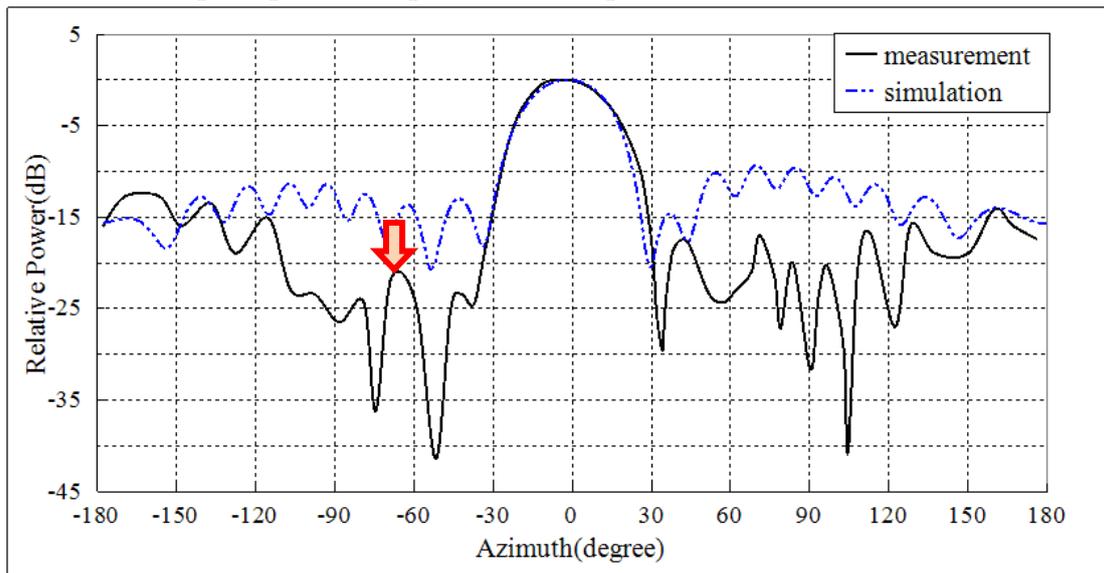
Figure 4-10 H-plane pattern comparison of the V-polarized 432MHz antenna

From the above figures, we find that the primary lobes of the measured patterns are in excellent agreement with the simulations. But in the side lobe region, there are substantial differences. In figure 4-9 the region indicated by the red arrow is the result of a strong reflection, as shown by detailed analysis in following paragraphs; in the region of 60° to180° the measured side lobe level is higher than in the simulation, by about 5…10dB.

In figure 4-10 the red arrow indicates a region affected by same factor of figure 4-9, in the other region the measured side lobes are weaker than the simulation, by about 10dB.

The measured pattern in red arrow region in figure 4-9 is an obviously abnormal region, the shape of side lobe in this region is obviously different from the simulated pattern, and the side lobe level is higher than the simulated pattern.

The following photo was taken on the roof of ISU near the signal generator and looking towards the Ground Station antenna. Next to the antenna one notes the vertical metal rod of the lightning protector. Because the radio signal from the signal generator is vertically polarized, the lightning rod can strongly reflect the signal to the Ground Station antenna.

Figure 4-11 The measurement environment on the roof

The following diagram shows the relative position of Ground Station antenna, signal generator antenna and reflection point. Angle A is obviously less than angle B, which means when we rotate the Ground Station antenna from the direction of signal generator antenna to reflection point, the primary lobe of 432MHz antenna will first reach the direction of reflection point. When we look back to Figures 4-9 and 4-10, we can find the abnormal region in the 144MHz antenna pattern is at -100°, and in 432MHz antenna pattern it is at -70°, so the abnormal region is affected by reflection.

On the right of following figure is column electromagnetic wave scattering diagram [Reference 9], the red arrow is the direction of the incoming wave and blue curve is the capability of reflection into different directions. When the angle from input direction to output direction is greater the reflection signal is weaker. Because angle C is greater than angle D, the reflected signal at 432MHz will be weaker than the reflected signal at 144MHz. The results of measurement show that the 144MHz antenna received the stronger reflected signal, again conform with the analysis.

The other important factor is the phase of the reflected signal: if the phase is same as that of the direct signal, the total signal will be stronger than normal, but if the phase difference is π, the total signal will be obviously weaker than normal. The phase difference of the reflected signal and the direct signal is determined by the path difference. If this path difference is an odd number of half-wavelengths the phase difference will be π, and if it is an even number of half-wavelengths, the phase of the reflected signal and the direct signal will be same.
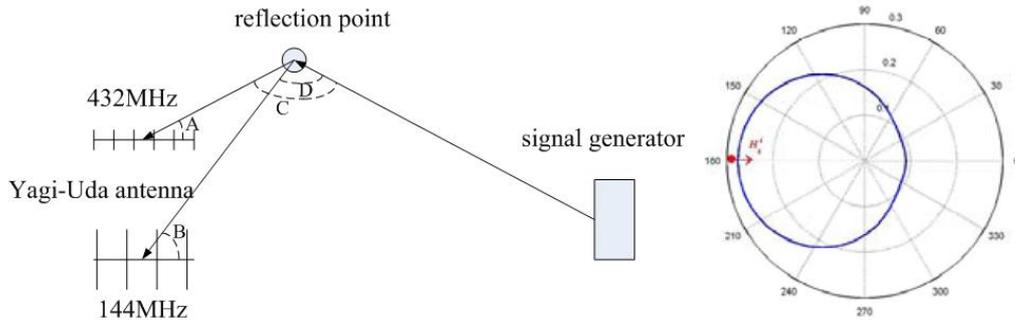
Figure 4-12 Measurement environment & electromagnetic wave scattering diagram

4.4. Measured antenna pattern in V-plane and comparison

Figures 4-14 and 4-15 are comparisons of measured and simulated patterns in the V-plane.

The relative positions of ISU ground station antenna and signal generator antenna are shown in the following diagram: the signal generator's antenna is lower than ground station antenna. Because the minimum elevation of the ground station antenna is 0°, so in fact the vertical plane pattern was measured from α to 180°+α with α≈5°. In Figures 4-14 and 4-15, the patterns have been compensated for this angle α.

Normally elevations are from 0° to 90°, but in Figures 4-14 and 4-15 we show the elevation from 0° to 180°: elevations greater than 90° indicate that the azimuth has been changed by 180° and the pattern at the antenna's rear side is shown. E.g. by supposing the azimuth is A when elevation is 10°, the elevation is 170° means the azimuth is A+180°, and actually the true elevation is 10°.
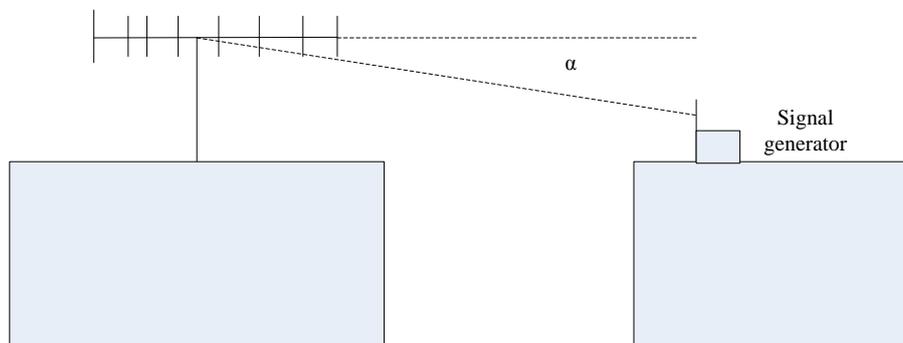
Figure 4-13 The relative positions of the antenna and signal generator
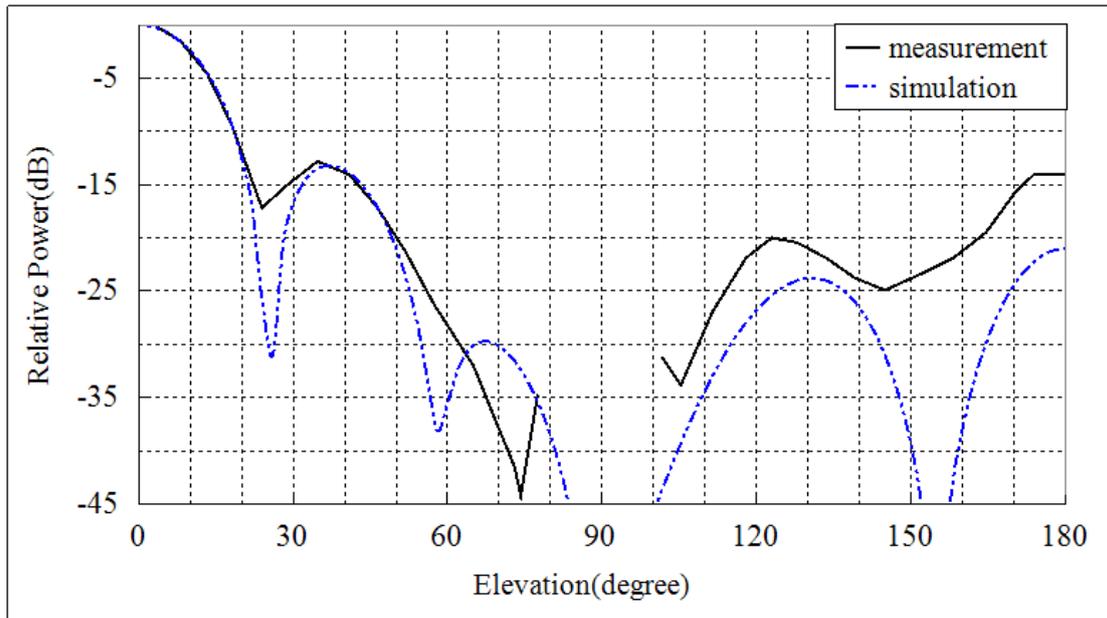
Figure 4-14 V-plane pattern comparison for the V-polarized 144MHz antenna
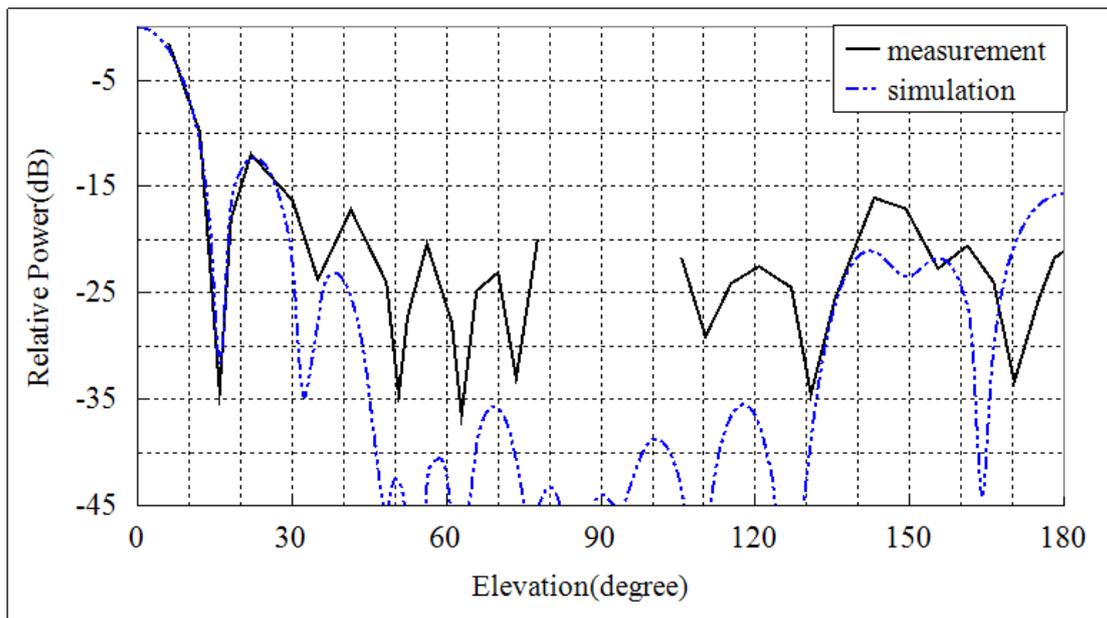
Figure 4-15 V-plane pattern comparison of the V-polarized 432MHz antenna

From two above figures, we find that the primary lobe and the first side lobe of measured patterns are conform with the simulated ones. In other regions, side lobes of measured patterns are different from the simulated ones.

Because the highest elevation of Ground Station antenna can reach is 80°, in Figures 4-14 and 4-15 the region from 80° to 100° is empty, without any measured data.

In Figure 4-14 we find that the region from 100° to 180°, the shape of side lobe of measured pattern is similar to simulated one, but the measured side lobe level is obviously higher than simulated one, in peak regions the difference is about 5dB, and in null regions the difference is more than 20dB.

In Figure 4-15 the shape of the side lobe of the measured pattern is not so similar to the simulated one as in Figure 4-14, the side lobe level of the measured pattern is higher than the simulated one by 5…20dB.

5. Reflection simulation and analysis

The ISU Ground Station antenna is fixed on the roof of the building, and the roof is not an ideal environment for antenna measurement, because the reflections from surrounding metal structures produce field variations in the test zone as the direct and reflected waves interfere.

Even small reflected signal may cause obvious influences on the measurements, especially in the side lobe region. If the reflected signal and the direct signal are all received through side lobe, the strength of direct signal and reflected signal may at same level. If the phase of reflected signal is same to direct signal, the power level will enhance by 6dB, if the phase difference of reflected signal and direct signal is 180°, there will be a null in measured pattern. The more serious case is when the reflected signal is received through the primary lobe but the direct signal is received through a side lobe like in the scenario of the lightning rod reflection, which has been analyzed in chapter 4.

The other important factor is reflection from the metal platform, because in most antenna measurement activities the reflection from a platform or the ground is a main factor. The following figure is a sketch of the roof of the ISU building. From the chapter 4, we find in all measured pattern that the side lobes are different from the simulations, how does the platform affect the measured pattern? The simulation software MMANA-GAL has a function of adding a ground plane to the model, so in order to find the answer some simulations about reflection have been done.
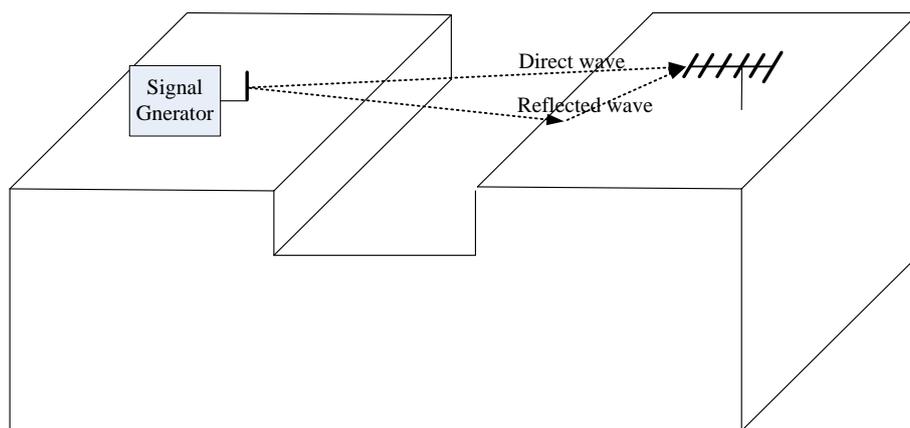
Figure 5-1 The situation of reflection by the roof

Because the reflection from the platform only affects the V-plane pattern, the simulation suffices to be in elevation.

MMANA-GAL has a function of selecting the type of a ground plane as perfect ground or real ground, at a specified height from platform to antenna. Perfect ground means the plane consists of perfectly conducting metal and the area is infinitely large. Real ground needs the input of dielectric constant, conductivity, and the size of the area.

The following table is from the help of MMANA-GAL, and shows the recommended values for dielectric constant and conductivity.

Ground	Dielectric constant	Conductivity (mS/m)
Sea water	81	4000
Fresh water	80	1 - 10
Wet ground	5 - 15	1 - 10
Dry field, forest	13	5
Sandy field	12	2
Suburb, industrial	5	1
Arid field	2 - 6	0.1

Table 5-1 Dielectric constant and conductivity of the ground

Because it was raining when we measured the Ground Station antenna, so the values of dielectric constant and conductivity were selected as Wet ground.Thus the simulation input parameter are as following:

Height: 2.14m

Dielectric constant: 10

Conductivity: 5

Area: 20m×20m

The following two figures are results of simulation in different conditions compared to the actual measurement.
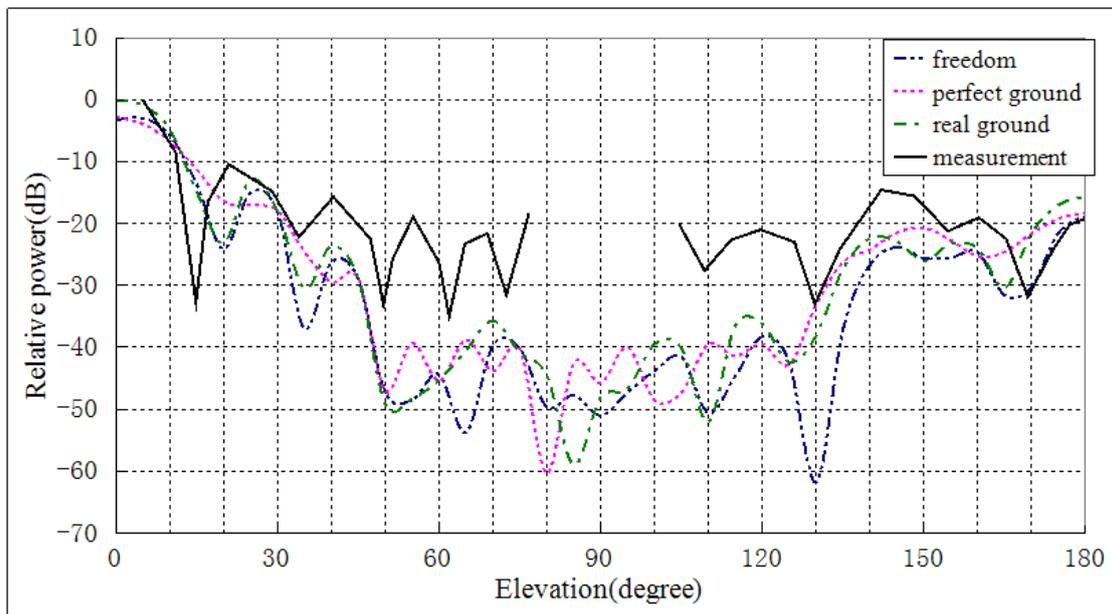
Figure 5-2 Comparison of measured and simulated patterns of the 432MHz antenna
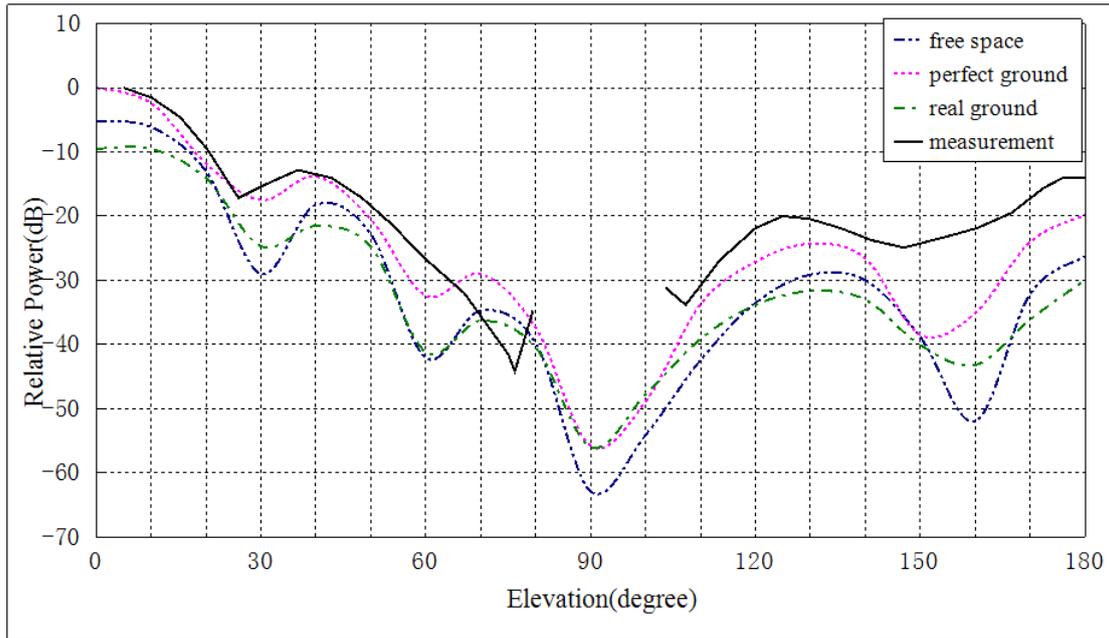
Figure 5-3 Comparison of measured and simulated patterns of the 144MHz antenna

From the above figures, we find that no single simulation curve is entirely consistent with the actual measurements. In figure 5-2 the simulated curves are different from each other in the side lobe region, which indicates that when one adds a reflective platform under the antenna, the antenna pattern should be changed, and different platforms will result in different patterns. But in figure 5-3 the simulated curves are not so different likes in figure 5-2, the possible reason is that the shorter wavelength is the more sensitive to reflection, and the 144MHz antenna is somewhat lower than the 432MHz antenna.

The reflection from platform seems not the main factor explaining the difference of measured and simulated patterns in the side lobe regions. A possible reason could be reflection from the guardrail.

6.   Summary of results

In this project the main work includes measuring the geometry of the antenna, constructing models of them, and measuring their radiation patterns. The result of the simulations is conforming to the analysis, the main characteristics of the antennas have been found out. Comparison of simulated and measured patterns shows that the primary lobes are in excellent agreement, but in the side lobe region there exist some differences, including the shape and the level of the side lobes. The main reason for these differences is very likely reflection. The most obvious effect comes from the strong reflection by the lightning rod.

The following figures are the results of simulation and measurement. Because the measured HPBW is very close to simulation, the table shows only one value.

Antenna	HPBW in H plane	HPBW in V plane	FBR (simulation)	FBR (measurement)
432MHz H-polarized Antenna	26°	14°	17dB	——
432MHz V-polarized Antenna	28°	14°	15dB	12dB
144MHz H-polarized Antenna	46°	22°	20dB	——
144MHz V-polarize Antenna	56°	22°	21dB	10dB

Table 6-1 Main characteristics of the Ground Station antenna

7. Conclusions and Recommendations

The goal of this project was to simulate and measure ISU Ground Station's 432MHz and 144MHz antennas, and to analyze the main factors that influence the actual antenna measurements.

The main conclusions are:

1) Even in a non-ideal environment, antenna measurement is useful, reliable information on the primary lobe is obtainable, but if information about the side lobe region is required, the antenna surroundings must contain no strong reflection points, especially metal objects.

2) Any metal rods near an antenna will seriously influence its pattern.

3) The simulation software MMANA-GAL is very useful; description of large antenna structures may be more efficient by directly editing the *.maa file.

The main recommendations are:

1) With the present software of ISU Ground Station, it is not possible to record attitude information, which caused low efficiency. If in the future the finer angle stepping is to be considered, it would be useful if an additional facility existed to automatically identify and record the information of azimuth and elevation.

2) For an actual antenna measurement one must avoid any metal objects near the antenna, if the antenna and metal objects are fixed, absorbing materials might be used to cover the metal objects.

3) For future studies, a small tower or ladder can be used to raise the antenna of signal generator to obtain improved results.

8. References

1. John D.Kraus, Ronald J.Marhefka, 2001, Antennas for all application, McGraw-Hill, New York, USA ,pp.835-854.

2. Lamont V.Blake, Maurice W.Long, 2008, Antennas: Fundamentals, Design, Measurement, Scitech, USA, pp.93~97, 371~392.

3. Fenglei Wu, Observation of Satellites with the ISU Ground Station. [Online]. Available from: http://astro.u-strasbg.fr/~koppen/ISU/FengleiReport.pdf   [Accessed 10April2013]

4. Voormansik, K., 2009. Satellite Signal Strength Measurements with the International Space University Ground Station and the University of Tartu Ground Station, Thesis (Master), UNIVERSITY OF TARTU.

5. Esteves, P., Köppen, J., 2010, The Ground Station's hardware. [Online]. Available from: http://astro.u-strasbg.fr/~koppen/GENSO/hardware.html   [Accessed 15 March 2013]

6. WIKIMEDIA COMMONS, 2010, P-18M radar. [Online].   Available from: http://commons.wikimedia.org/wiki/File:P-18M_radar.jpg   [Accessed 19 April 2013]

7. REMC, Antenna Measurement Chamber, [Online].   Available from: http://www.rainfordemc.com/antenna-measurement-chamber.html   [Acc'd 15April 2013]

8. Comba, 2009，天线测试操作培训，p.10, [Online].   Available from: http://wenku.baidu.com/view/5a3b70e9b8f67c1cfad6b8d7   [Accessed 14 April 2013]

9. Ming-Tse Liu, Scattering of a Plane Electromagnetic Wave by a Conducting Cylinder, Journal of Yuanpei University, Taiwan, December 2009, No.16.

9. Appendices
9.1. The model of V-polarized 432MHz antenna
The model of V-polarized 432MHz antenna

*

432.0

Wires

36

-0.689,   0.0, -0.483,   -0.689,   0.0, -0.807,   0.0025, -1
-0.696,   0.028,   -0.486,   -0.696,   0.028,   -0.804,   0.0015, -1
-0.689,   0.0, -0.5015, -0.696,   0.028,   -0.5015, 0.003,   -1
-0.689,   0.0, -0.7945, -0.696,   0.028,   -0.7945, 0.003,   -1
-0.652,   0.0, -0.4885, -0.652,   0.0, -0.8015, 0.0025, -1
-0.518,   0.0, -0.4925, -0.518,   0.0, -0.7975, 0.0025, -1
-0.363,   0.0, -0.5,-0.363,   0.0, -0.79,   0.0025, -1
-0.211,   0.0, -0.4985, -0.211,   0.0, -0.7915, 0.0025, -1
0.0, 0.0, -0.5,0.0, 0.0, -0.79,   0.0025, -1
0.198,   0.0, -0.505,   0.198,   0.0, -0.785,   0.0025, -1
0.407,   0.0, -0.5035, 0.407,   0.0, -0.7865, 0.0025, -1
0.648,   0.0, -0.505,   0.648,   0.0, -0.785,   0.0025, -1
0.893,   0.0, -0.508,   0.893,   0.0, -0.782,   0.0025, -1
1.129,   0.0, -0.508,   1.129,   0.0, -0.782,   0.0025, -1
1.396,   0.0, -0.508,   1.396,   0.0, -0.782,   0.0025, -1
1.663,   0.0, -0.508,   1.663,   0.0, -0.782,   0.0025, -1
1.909,   0.0, -0.5015, 1.909,   0.0, -0.7885, 0.0025, -1
-0.842,   0.0, -0.4825, -0.842,   0.0, -0.8075, 0.0025, -1
-0.689,   0.0, 0.807,   -0.689,   0.0, 0.483,   0.0025, -1
-0.696,   0.028,   0.804,   -0.696,   0.028,   0.486,   0.0015, -1
-0.689,   0.0, 0.7885, -0.696,   0.028,   0.7885, 0.003,   -1
-0.689,   0.0, 0.4955, -0.696,   0.028,   0.4955, 0.003,   -1
-0.652,   0.0, 0.8015, -0.652,   0.0, 0.4885, 0.0025, -1
-0.518,   0.0, 0.7975, -0.518,   0.0, 0.4925, 0.0025, -1
-0.363,   0.0, 0.79,   -0.363,   0.0, 0.5, 0.0025, -1
-0.211,   0.0, 0.7915, -0.211,   0.0, 0.4985, 0.0025, -1
0.0, 0.0, 0.79,   0.0, 0.0, 0.5, 0.0025, -1
0.198,   0.0, 0.785,   0.198,   0.0, 0.505,   0.0025, -1
0.407,   0.0, 0.7865, 0.407,   0.0, 0.5035, 0.0025, -1
0.648,   0.0, 0.785,   0.648,   0.0, 0.505,   0.0025, -1
0.893,   0.0, 0.782,   0.893,   0.0, 0.508,   0.0025, -1
1.129,   0.0, 0.782,   1.129,   0.0, 0.508,   0.0025, -1
1.396,   0.0, 0.782,   1.396,   0.0, 0.508,   0.0025, -1
1.663,   0.0, 0.782,   1.663,   0.0, 0.508,   0.0025, -1
1.909,   0.0, 0.7885, 1.909,   0.0, 0.5015, 0.0025, -1
-0.842,   0.0, 0.8075, -0.842,   0.0, 0.4825, 0.0025, -1

Source

2,   0

w2c,   0.0, 1.0
w20c,   0.0, 1.0
Load
0,   1
Segmentation
200, 20,   2.0, 2
G/H/M/R/AzEl/X
0,   2.14,   0,   50.0,   120, 60,   0.0

9.2. The model of V-polarized 144MHz antenna

The model of V-polarized 144MHz antenna
*
144.0
Wires
20
-0.608,   0.0, -0.7185, -0.608,   0.0, -1.7215, 0.0025, -1
-0.603,   -0.019, -0.7185, -0.603, -0.019, -1.7215, 0.003,   -1
-0.608,   0.0, -0.7185, -0.603, -0.019, -0.7185, 0.003,   -1
-0.608,   0.0, -1.7215, -0.603, -0.019, -1.7215, 0.003,   -1
-0.471,   0.0, -0.7495, -0.471,   0.0, -1.6905, 0.0025, -1
-0.148,   0.0, -0.748, -0.148,   0.0, -1.692, 0.0025, -1
0.405,   0.0, -0.759, 0.405,   0.0, -1.681, 0.0025, -1
1.109,   0.0, -0.7755, 1.109,   0.0, -1.6645, 0.0025, -1
1.808,   0.0, -0.7775, 1.808,   0.0, -1.6625, 0.0025, -1
-0.858,   0.0, -0.71,   -0.858,   0.0, -1.73,   0.0025, -1
-0.608,   0.0, 1.7215, -0.608,   0.0, 0.7185, 0.0025, -1
-0.603,   -0.019, 1.7215, -0.603, -0.019, 0.7185, 0.003,   -1
-0.608,   0.0, 1.7215, -0.603, -0.019, 1.7215, 0.003,   -1
-0.608,   0.0, 0.7185, -0.603, -0.019, 0.7185, 0.003,   -1
-0.471,   0.0, 1.6905, -0.471,   0.0, 0.7495, 0.0025, -1
-0.148,   0.0, 1.692, -0.148,   0.0, 0.748,   0.0025, -1
0.405,   0.0, 1.681, 0.405,   0.0, 0.759,   0.0025, -1
1.109,   0.0, 1.6645, 1.109,   0.0, 0.7755, 0.0025, -1
1.808,   0.0, 1.6625, 1.808,   0.0, 0.7775, 0.0025, -1
-0.858,   0.0, 1.73,   -0.858,   0.0, 0.71,   0.0025, -1
Source
2,   0
w2c,   0.0, 1.0
w12c,   0.0, 1.0
Load
0,   1
Segmentation
200, 20,   2.0, 2
G/H/M/R/AzEl/X
0,   2.14,   0,   50.0,   120, 60,   0.0

27

9.3. The calibration data of 144MHz receiver

Power of input signal (dBm)	Code receiver output
-120	3
-115	5
-110	67
-105	96
-100	115
-95	129
-90	141
-80	161
-70	183
-60	203
-55	215
-50	227

Table 9-1 The calibration data of 144MHz receiver

9.4. The calibration data of 432MHz receiver

Power of input signal (dBm)	Code receiver output
-120	3
-115	31
-110	76
-105	101
-100	122
-95	133
-90	146
-80	168
-70	190
-60	212
-50	237

Table 9-2 The calibration data of 432MHz receiver

9.5. Antenna parameter measurement

9.5.1. H-polarized 432MHz Antenna

The relative positions of wires are as in the following diagram.
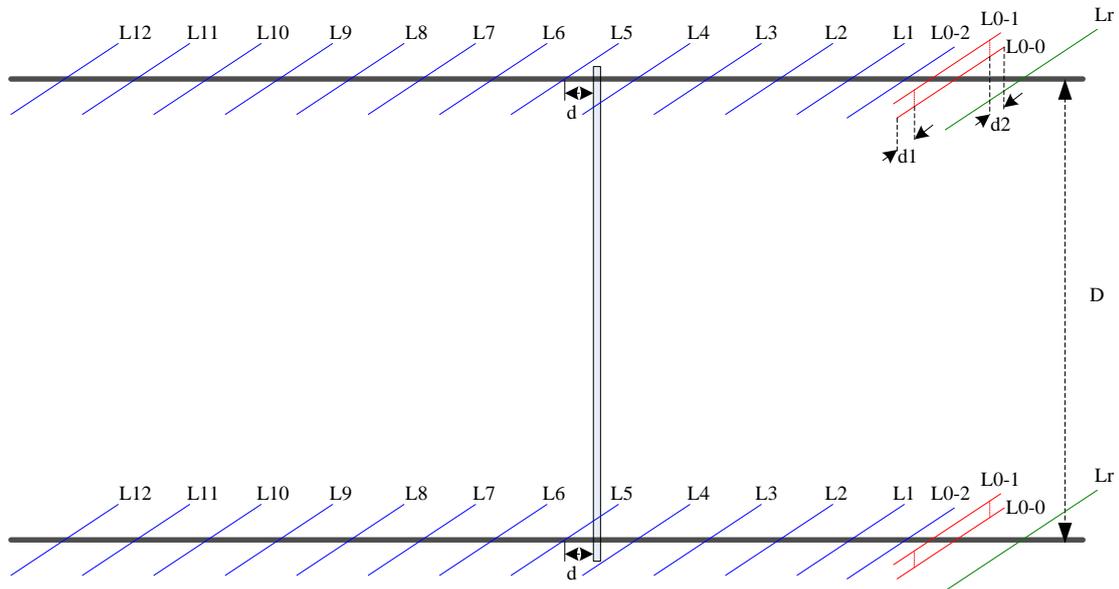
Figure 9-1 The diagram of the H-polarized 432MHz antenna

The parameters of the antenna are listed in the following table.

Wire	Length(cm)	Diameter(cm)	Distance to L0-0(cm)		
			axial direction	Vertical	
L0-0	34.4	0.5	0	0	active
L0-1	31.5	0.3	1	2.7	active
L0-2	31.2	0.5	3.6	0	
Lr	32.6	0.5	15.8	0	
L1	30.5	0.5	17.7	0	
	Length(cm)	Diameter(cm)	Distance to Ln-1(cm)		
L2	29	0.5	14.3	0	
L3	29.4	0.5	15.3	0	
L4	29	0.5	20.9	0	
L5	28	0.5	19.9	0	
L6	28.2	0.5	20.9	0	
L7	28	0.5	24	0	
L8	27.5	0.5	24.4	0	
L9	27.2	0.5	23.7	0	
L10	27.5	0.5	26.5	0	
L11	27.5	0.5	27.1	0	
L12	28.9	0.5	25.2	0	
D	129cm		d1	2.2cm	
d	12.2cm		d2	2.4cm	

Table 9-3 The parameters of the H-polarized 432MHz antenna

9.5.2. V-polarized 432MHz Antenna

The relative positions of wires are as in the following diagram.
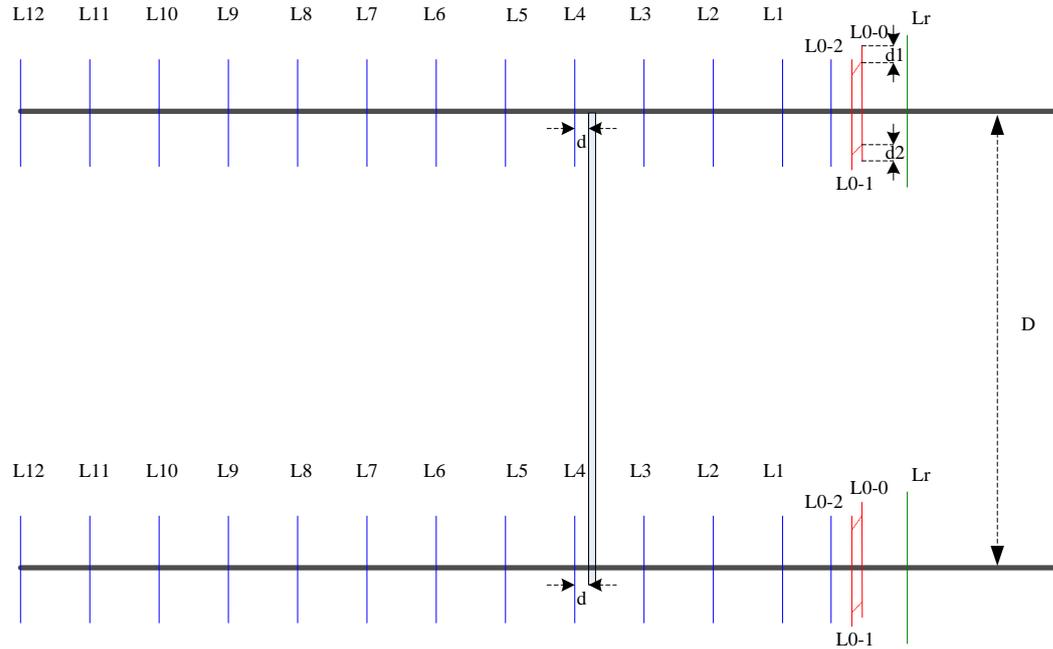
Figure 9-2 The diagram of the V-polarized 432MHz antenna

The parameters of the antenna are listed in the following table.

Wire	Length(cm)	Diameter(cm)	Distance to L0-0(cm)		
			axial direction	Vertical	
L0-0	32.5	0.5	0	0	active
L0-1	31.8	0.3	0.7	2.8	active
L0-2	31.3	0.5	3.7	0	
Lr	32.5	0.5	15.3	0	
L1	30.5	0.5	17.1	0	
	Length(cm)	Diameter(cm)	Distance to Ln-1(cm)		
L2	29	0.5	15.5	0	
L3	29.3	0.5	15.2	0	
L4	29	0.5	21.1	0	
L5	28	0.5	19.8	0	
L6	28.3	0.5	20.9	0	
L7	28	0.5	24.1	0	
L8	27.4	0.5	24.5	0	
L9	27.4	0.5	23.6	0	
L10	27.4	0.5	26.7	0	
L11	27.4	0.5	26.7	0	
L12	28.7	0.5	24.6	0	
D	129cm		d1	1.3cm	
d	9cm		d2	1.9cm	

Table 9-4 The parameters of the V-polarized 432MHz antenna

9.5.3. H-polarized 144MHz Antenna

The relative positions of wires are as in the following diagram.
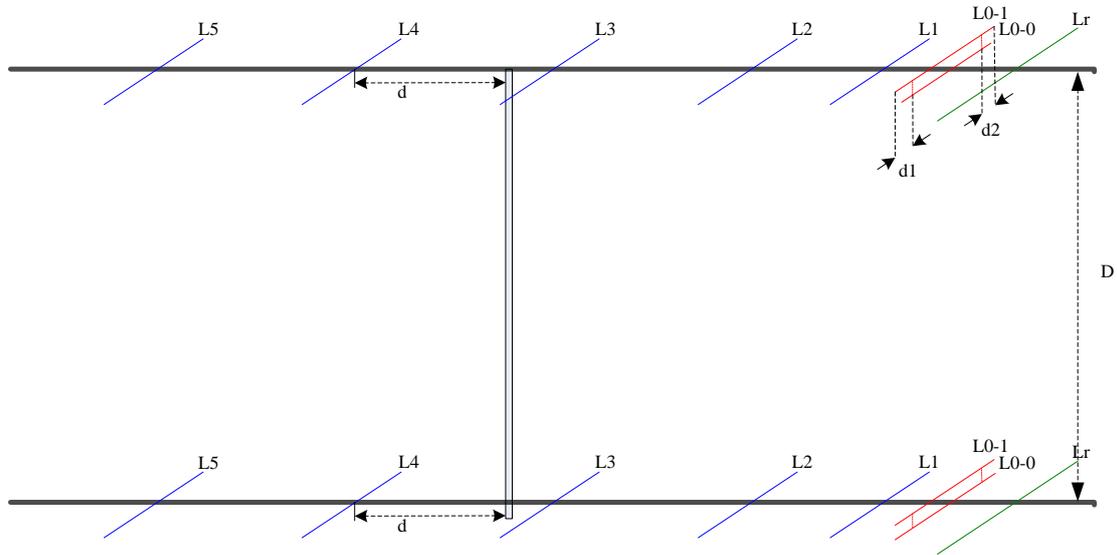
Figure 9-3 The diagram of the H-polarized 144MHz antenna

The parameters of the antenna are listed in the following table.

Wire	Length(cm)	Diameter(cm)	Distance to L0-0(cm)		
			axial direction	Vertical	
L0-0	100.5	0.5	0	0	active
L0-1	104.5	0.6	0.3	2.9	active
Lr	102	0.5	24.5	0	
L1	94.3	0.5	14.2	0	
	Length(cm)	Diameter(cm)	Distance to Ln-1(cm)		
L2	94.5	0.5	32.3	0	
L3	92.5	0.5	55.3	0	
L4	90	0.5	70.7	0	
L5	88.6	0.5	69.9	0	
D	244cm		d1	2.9cm	
d	61.5cm		d2	2cm	

Table 9-5 The parameters of the H-polarized 144MHz antenna

9.5.4. V-polarized 144MHz Antenna

The relative positions of wires are as in the following diagram.
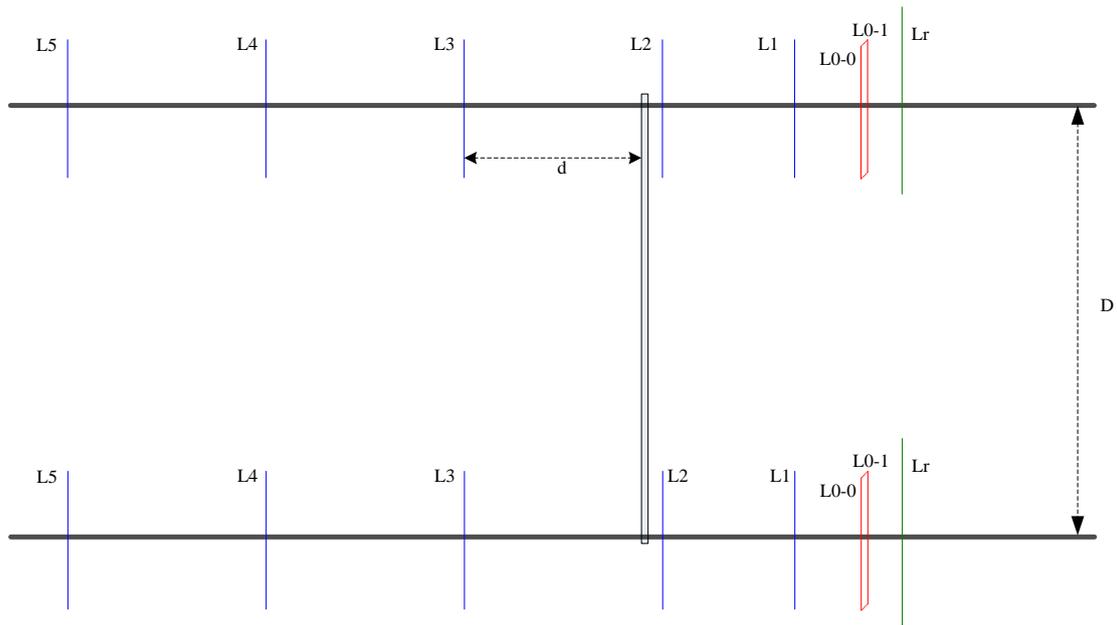
Figure 9-4 The diagram of the V-polarized 144MHz antenna

The parameters of the antenna are listed in the following table.

Wire	Length(cm)	Diameter(cm)	Distance to L0-0(cm)		
			axial direction	Vertical	
L0-0	100.3	0.5	0	0	active
L0-1	100.3	0.6	0.5	1.9	active
Lr	102	0.5	25	0	
L1	94.1	0.5	13.7	0	
	Length(cm)	Diameter(cm)	Distance to Ln-1(cm)		
L2	94.4	0.5	32.3	0	
L3	92.2	0.5	55.3	0	
L4	88.9	0.5	70.4	0	
L5	88.5	0.5	69.9	0	
D	244cm				
d	40.5cm				

Table 9-6 The parameters of the V-polarized 144MHz antenna